

An Underactuated Adaptive 3D Printed Robotic Gripper

Kuat Tlegenov, Yedige Tlegenov and Almas Shintemirov, *Member, IEEE*

Abstract – This paper presents the preliminary work on prototype design and analysis of a 3D printed three-fingered underactuated robotic gripper with a breakaway clutch mechanism. An underactuated mechanical design, kinematics of gripper's finger and a breakaway clutch mechanism are described in details. These elements provide passive adaptive object grasping and relatively high load carrying capacity of the gripper. The robotic gripper was prototyped using 3D printing technology and off-the-shelf components. Simulation and experimental results of grasping performance characterization of the robotic gripper are also presented.

I. INTRODUCTION

VARIOUS robotic end effectors were developed for wide range of applications where reproducing the human hand functionality is required [1-3]. In most of industrial and service applications manipulation of objects with anthropomorphic robotic hands is not compulsory and three fingered grasping devices are more sufficient [4]. Many

robotic grippers utilize individual actuation of each joint of the finger using a small high precision DC servomotors (Fig. 1(a, b)) [5][6]. This finger design provides high number of controllable degrees of freedom (DOFs), which is very suitable for grasping of complex shape objects. On the other hand, usage of multiple actuators in each finger mechanism results in high cost of the device and design complexity.

A number of designs utilize pulley/tendon driven mechanisms that are used for industrial and service robotic systems (Fig. 1(c, d)) [7][8]. These mechanisms have many advantages such as low cost due to less number of actuators, high degree of adaptability and universality for different applications; they have limited load carrying capacity. As an alternative, different designs of underactuated artificial fingers based on mechanical linkage systems are proposed (Fig. 1(e, f, g)) [9-11]. Above-mentioned end-effectors with mechanical linkage system are complex in their manufacturing and have high number of miniature parts. Thus, there is a need for an end effector, providing configurability for different range of

Mechanisms of artificial fingers and their applications in robotic hands



Fig. 1. High-speed multifingered hand (a), Schunk Hand (b), Barrett Hand (c), i-HY Hand (d), Delft Hand (e), Robotiq Gripper (f), Kinova JACO Gripper (g).

Manuscript received June 30, 2014. This work was supported by the Kazakhstan Ministry of Education and Science under grant and target funding scheme (agreement #001-2014).

All authors are with Department of Robotics and Mechatronics, School of Science and Technology and Nazarbayev University Research and Innovation System, Nazarbayev University, Astana, Kazakhstan 010000 e-mails: {ktelegenov, yedige.tlegenov, ashintemirov}@nu.edu.kz.

gripping operations with high degree of wear and shock resistance, relatively high payload, simple control systems, and simple mechanical structures [12].

Applications of the concept of adaptive mechanical system in the design of robotic devices have been studied recently

[13]. In this paper, authors present their preliminary work on design and analysis of an underactuated adaptive robotic three fingered end effector. An important characteristic of the presented gripper is the provision of underactuation within each finger and between the fingers provides fully enveloping of the object without detailed prior knowledge of its shape. Underactuation between fingers is achieved by using a breakaway clutch mechanism, which has novel application to grippers and robotic end effectors.

The organization of the paper is as follows. Section II describes design of a two DOFs underactuated finger mechanism and a breakaway clutch mechanism. Section III presents the design of a three-fingered robotic gripper. The grasping performance and simulation of the robotic gripper prototype are analyzed in Section IV, which is followed by the conclusions and future directions of work.

II. DESIGN OF THE UNDERACTUATED FINGER AND BREAKAWAY CLUTCH MECHANISM

A. Underactuated Finger Mechanism

Underactuated fingers have less number of actuators than totals DOFs and are widely utilized in designs of various robotic hands for industrial [14] and service robotics [15]. This is largely attributed to the relatively simple design of such mechanisms comparing with fully actuated dexterous artificial fingers. The underactuated finger mechanism ensures close wrapping of different shape objects due to its adaptive grasping capability with one actuator.

In this work, the underactuated linkage mechanism is employed for finger design [16][17]. This ensures simple low-cost mechanical system which is one of the principles of finger design requirements [18]. The proposed gripper has two degrees-of-freedom (2-DOF) and one degree-of-actuation (1-DOA) in each underactuated finger mechanism. To provide actuation of the second DOF a passive element, i.e. a spring, is used between first and second finger phalanges [17].

The finger design layout is presented in Fig. 2a and consists of two phalanges, two links, a spring and a worm wheel. Note that the worm wheel and the link 1 have rigid connection. The worm wheel is transmitting rotary motion to the link 1 about its pivot point; following link 1 transfers the motion to the link 2.

The spring allows the finger to behave as a single rigid body in rotary motion about a fixed pivot. When the first phalanx meets with an object, the force produced by actuator extends the spring, which starts transferring motion to the second phalanx only. The contact of two phalanges with a grasping object represent the last stage of a closing sequence.

In overall, the underactuated finger design provides relatively high load carrying capacity comparing to similar tendon driven mechanisms and requires minimum number of actuators in the gripper. This with utilization of off-the-shelf components and 3D printing technology ensures lower cost, simple control effort and less weight of the gripper prototype.

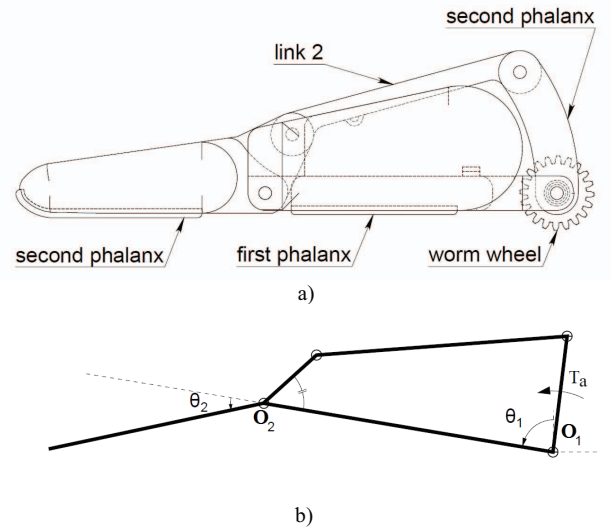


Fig. 2. (a) 2D design of the underactuated finger (b) and its schematic model

B. 2-DOF 1-DOA Finger Analysis

In order to define the stiffness of the spring K_1 which provides actuation of the finger second phalanx, the kinematic analysis of the finger mechanism with a linkage system is presented below. The schematic model of the finger is shown in Fig. 2b.

The quasi-static modelling of the finger is defined as follows. By equating the input and the output virtual powers [4], the following expression is derived

$$t^T \omega_a = f^T v. \quad (1)$$

Where t is the input torque vector, ω_a is the velocity vector, f is the vector of contact wrenches, and v is the vector containing the twist of contact points [19], which are defined as follows:

$$t = \begin{bmatrix} T_a \\ T_2 = -K_1 \Delta \theta_2 \end{bmatrix}; \quad \omega_a = \begin{bmatrix} \dot{\theta}_{a1} \\ \dot{\theta}_2 \end{bmatrix}; \quad (2)$$

$$f = \begin{bmatrix} \zeta_1^\circ \\ \zeta_2^\circ \end{bmatrix}; \quad v = \begin{bmatrix} \xi_1 \\ \xi_2 \end{bmatrix}, \quad (3)$$

where T_a is the actuation wrench, K_1 is the stiffness of the spring, $\dot{\theta}_i$ is first derivative of the phalanx joint coordinates, ζ_i° is a shorthand for row vector $\zeta_i^\circ = [m_z f_i^x f_i^y]$ found from three-dimensional vector of the wrench $\zeta_i = [f_i^x f_i^y m_z]$ by writing the moment before the force coordinates, where $f_i = (f_i^x f_i^y)$ is a unit vector parallel to the force and m_i is the moment of the force axis about the platform center [20]. ξ_i is the three-dimensional vector $\xi_i = [\omega_z \mathcal{Q}_i^x \mathcal{Q}_i^y]$ for planar twist.

Equation (1) then becomes

$$[T_a \quad -K_1 \Delta \theta_2] \cdot \begin{bmatrix} \dot{\theta}_{\alpha_1} \\ \dot{\theta}_2 \end{bmatrix} = [\zeta_1 \circ \quad \zeta_2 \circ] \cdot \begin{bmatrix} \xi_1 \\ \xi_2 \end{bmatrix}, \quad (4)$$

where by equating two matrixes from each side the following equation is obtained

$$T_a \times \dot{\theta}_{\alpha_1} - K_1 \Delta \theta_2 \times \dot{\theta}_2 = \zeta_1 \circ \times \xi_1 + \zeta_2 \circ \times \xi_2. \quad (5)$$

Thus, the stiffness of the spring can be expressed as

$$K_1 = \frac{T_a \times \dot{\theta}_{\alpha_1} - \zeta_1 \circ \times \xi_1 + \zeta_2 \circ \times \xi_2}{\Delta \theta_2 \times \dot{\theta}_2}. \quad (6)$$

Equation (6) defines the stiffness of the spring that provides the second DOF for the tip of the finger mechanism, and is used in further analysis of the robotic gripper mechanism design.

C. Breakaway Clutch Mechanism Analysis

In order to provide adaptive passive grasping of an object an underactuated robotic gripper with three fingers should actuate fingers independently from each other. In the presented design the use of a breakaway clutch mechanism with a single actuator is proposed for providing high underactuation of the three-fingered robotic gripper.

As all three fingers are driven by a single motor, the actuation is transmitted from the motor to the fingers through a series of gears. To achieve full wrapping of an object with three fingers by a single actuator, the underactuation principle is used between individual fingers for providing maximum grasp contact. If a finger is blocked by contact with an object, other fingers still move to complete their closing sequence.

In general, underactuation principle between fingers can be achieved using differential mechanisms. Various differential actuation mechanisms between fingers, such as gear differentials, linkage seesaw differentials, and pulley differentials can be applied [21][22]. Gear differential mechanisms result to relatively high space requirements whereas linkage seesaw and pulley differential systems have payload capacity limitations.

Previously, Ulrich [23] presented a novel breakaway clutch mechanism to accomplish enveloping grasping of three fingered end effector. However, the proposed mechanism is quite difficult to manufacture using a 3D printing technology due to low resolution of printing and low elastic modulus of printing materials.

To achieve compatibility with 3D printing technology, the robotic end effector design must have simple structural units and have minimal number of miniature parts. A novel breakaway clutch mechanism design for three fingered robotic gripper proposed in this paper is described below.

The architecture of a breakaway clutch mechanism for a single finger consists of two helical gears, a worm wheel, a worm and a compression spring, as shown in Fig. 3.

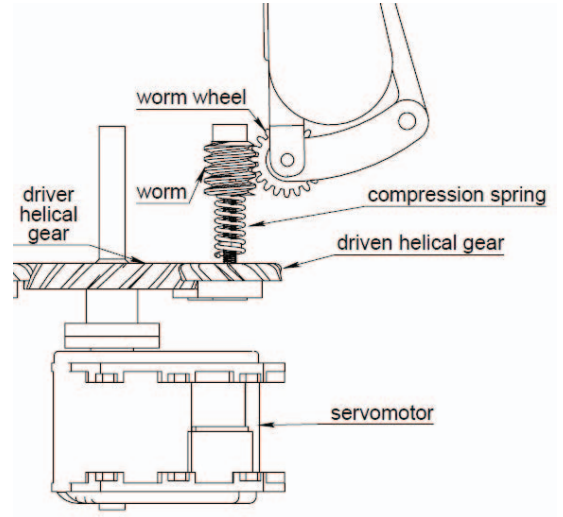


Fig. 3. 2D model of breakaway clutch mechanism.

The driver helical gear rotates the driven helical gear which in its turn drives the worm on the same shaft. The driven helical gear and the worm are rigidly connected with the shaft along their vertical axis. The worm transmits motion to the worm wheel, which is pivotally connected to the palm and transmits rotational motion to the finger. The 3D model of the clutch mechanism and its allocation in the palm is presented in Fig.4.

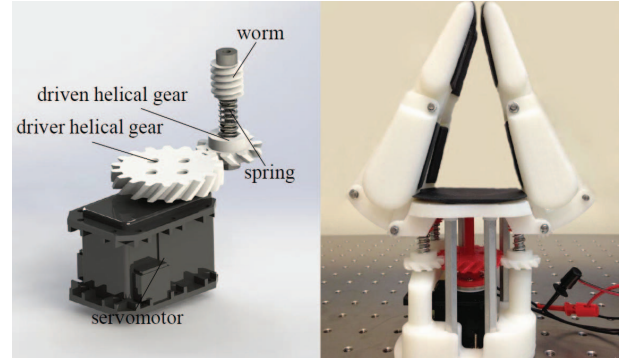


Fig. 4. A 3D model and a prototype of the proposed breakaway clutch mechanism.

The main reason of utilizing helical gears is that an axial thrust load is produced as a natural result of the inclined arrangement of teeth. The driven helical gear is able to slide along its vertical axis while rotation. The sliding movement is restricted by the compression spring located between the driven helical gear and the worm on the same shaft. Any sliding mechanism can be used for facilitating vertical smooth motion of the driven helical gear.

Analyzing forces acting on helical gear, shown in Fig. 5, it can be seen that axial force F_x acts in the tangential plane parallel to the axis of the shaft carrying the helical gear.

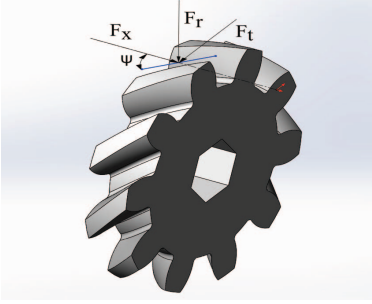


Fig. 5. Perspective view of geometry and forces of helical gear.

Axial force F_x tends to push the mating gear along the shaft and is computed as follows:

$$F_x = F_t \tan \psi, \quad (7)$$

where F_t is tangential or transmitted force and ψ is helix angle.

Force $F_t = \frac{2T}{D}$ is tangential to the pitch surface of the gear and is perpendicular to the axis of the shaft carrying the gear. T and D are transmitted torque and pitch diameter of the gear respectively. This is the force that actually drives the gear. ψ defines the angle that teeth are inclined with the axis.

Substituting F_t in equation (7) yields

$$F_x = \frac{2T}{D} \tan \psi. \quad (8)$$

Axial thrust load must be larger than the force exerted by the compression spring to start helical gear sliding upward along its axis. The spring force is

$$F_s = K_2 x, \quad (9)$$

where K_2 and x is the stiffness and displacement of the compression spring of the breakaway clutch mechanism, respectively.

By equating (8) to (9) the equilibrium equation for the breakaway clutch mechanism in vertical direction is obtained. Hence, the stiffness of the compression spring is defined as follows:

$$K_2 = \frac{2T}{Dx} \tan \psi. \quad (10)$$

The stiffness of the compression spring is the same for the clutches of three fingers in the designed robotic gripper.

III. DESIGN AND ANALYSIS OF 3D PRINTED THREE FINGERED ROBOTIC GRIPPER

A. Design and Fabrication

The three fingered robotic gripper includes the three 2 DOFs underactuated fingers, a frame housing a palm, the breakaway clutch mechanism and an actuator.

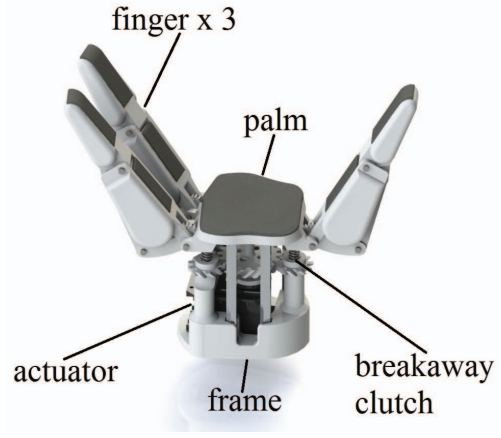


Fig. 6. 3D CAD model of the three-fingered robotic end effector.

The arrangement of the fingers allows the gear trains of the fingers to be driven from a single actuator. Two fingers are placed opposite to each other and the third finger is adjusted to one of them. The two opposite fingertips are designed to be able to grasp tiny objects.

Each gripper finger has the breakaway clutch mechanism discussed in Section II. This mechanism contains a worm wheel that enables self-locking property of each finger in their closing and opening sequence when the actuator is powered off [23].

The CAD design of the robotic gripper is presented in Fig. 6, whereas the gripper prototype is shown in Fig. 4. The gripper prototype is fabricated using a 3D rapid prototyping technology using ABS plastic and rubber materials with use of additional off-the-shelf components.

A Dynamixel MX-28 servomotor is used as an actuator for robotic gripper prototype. This allows eliminating complex electronic circuits and encoders for motor position control. Control of the actuator is performed from Robot Operating System (ROS), which makes integration with other ROS-based systems easy and straightforward.

Combining the finger and the breakaway clutch mechanisms into a single system requires selecting appropriate parameters for the springs. To provide proper grasping of an object, underactuation within the finger have to be activated to perform full wrapping, following by underactuation between the fingers. This can be achieved if the stiffness of the spring in the clutch is larger than the stiffness of the spring in the finger as presented below

$$K_1 \leq K_2. \quad (11)$$

In order to work properly the springs in the fingers and in the breakaway clutch must be preloaded.

The actuation wrench T_a is applied to the pivot point of the finger, transferring rotational motion. In the presented design with one actuator and three fingers the actuation wrench of each finger can be calculated knowing the transmitted torque T as follows:

$$T_a = \frac{\zeta_1 \circ \times \zeta_1 - \zeta_2 \circ \times \zeta_2}{\dot{\theta}_{\alpha_1}} + \frac{2T \times \Delta\theta_2 \times \dot{\theta}_2}{Dx \times \dot{\theta}_{\alpha_1}} \tan \psi. \quad (12)$$

Thus, the design parameters for the actuation wrench with respect to the applied torque applied from the output shaft of the motor are defined. In the robotic gripper prototype the output shaft of the Dynamixel actuator is directly connected to an 18 teeth helical gear with 1.5 inches pitch diameter, which drives three smaller 10 teeth helical gears, with 0.833 inches pitch diameter, one for each finger mechanism. The three helical gears are rotating together with three worms, with 1 thread and 0.8 module. Finally, the three worms transfer rotational motion to three 20 teeth worm wheels with 0.62 inches pitch diameter, which are connected to the fingers. The output torque of Dynamixel MX-28 servomotor is 2.5 Nm at 12V power supply voltage [24].

IV. GRASPING PERFORMANCE AND SIMULATION

The main grasping patterns of the robotic gripper can be summarized to three main configurations: cylindrical, spherical and planar [25], as illustrated in Fig. 7. All three fingers of the robotic gripper are pivoted to the palm in a way that allows perform the grasping configurations without changing orientation of the finger base. This simplifies the gripper design due to excluding possible mechanisms for changing the finger orientations and additional actuators.

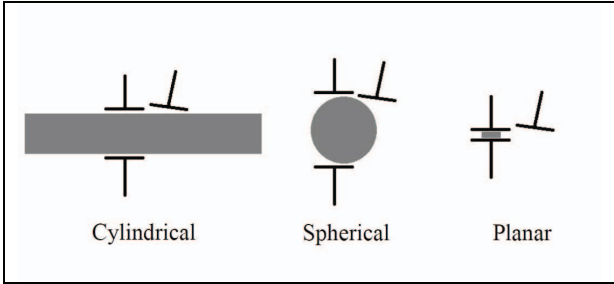


Fig. 7. Main grasping configurations.

The analysis of grasping performance of the gripper is carried out by simulation using ADAMS mechanical system modeling software. The kinematic model of the finger shown in Fig. 2b is simulated to analyze the dependence of the gripping force at the fingertip from the input actuator torque.

Fig. 8 illustrates the performance of the proposed robotic gripper in grasping a number of objects with different shapes. It is seen that gripper fingers adapt to the shape of objects. For instance, in the spherical grasping the gripper almost fully envelops a ball object. The planar grasping is performed at the fingertips using all three fingers, whereas the fingertip grasp utilizes only two fingers for picking up small objects. The video of the gripper performance is available on www.alaris.kz.

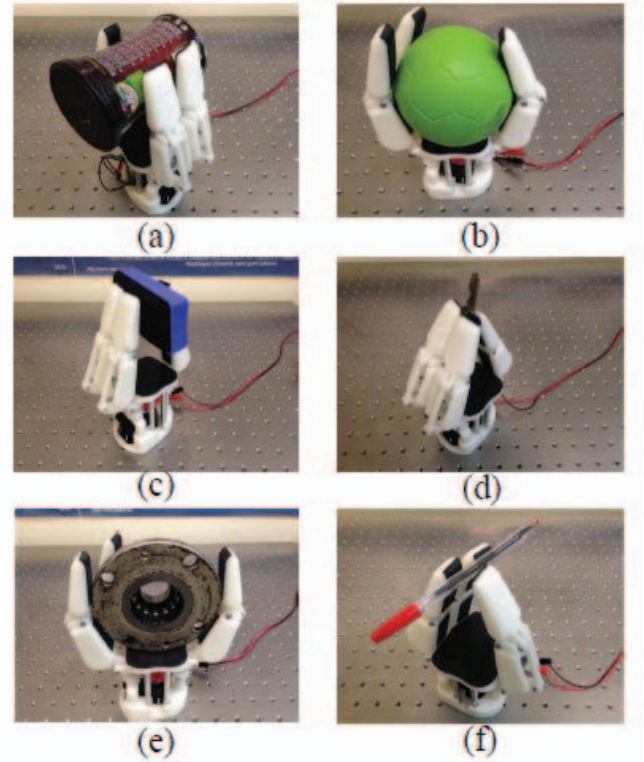


Fig. 8. Grasping of different objects of the robotic gripper prototype: (a) Cylindrical grasp. (b) Spherical grasp. (c) Planar grasp. (d) Fingertip grasp. (e) High payload, large shape grasp. (f) Low payload, small shape grasp.

The simulation results are confirmed experimentally using the robotic gripper prototype as shown in Fig. 9. It can be clearly seen that there is a slight difference of the gripping force between experimental and simulation results which might be attributed to energy loss between moving parts of the gripper prototype.

The experimental test are performed using a force gauge for measuring applied gripping force at the fingertip. The tests show that maximum gripping force of the presented robotic gripper reaches 15 N. However, due to non-backdriveability of the gripper actuating mechanism, the fingers may resist much larger forces that they actually exert [12].

A comparison of the proposed robotic gripper with widely applied robotic end effectors is presented in Table I. All the compared robotic end effectors have three-fingered design. However, they were developed for different purposes and applications, such as industrial (Barrett Hand, Robotiq, Schunk SDH Hand) or service (Kinova JACO, i-HY Hand) use. A number of utilized actuators is an important parameter contributing to the cost of a robotic end effector. As clear from Table I the proposed gripper design shows comparable gripping force characteristics. The use of the minimum number of actuators and 3D printing technology makes the proposed gripper potentially preferable in terms of the cost to payload ratio.

However, 3D printing is primarily a prototyping technology, thus parts are created for test purposes. The printing accuracy

cannot be ignored while choosing dimensions for different parts of the gripper. Low resolution of printing and low elastic modulus of the printed materials also should be taken into account during design.

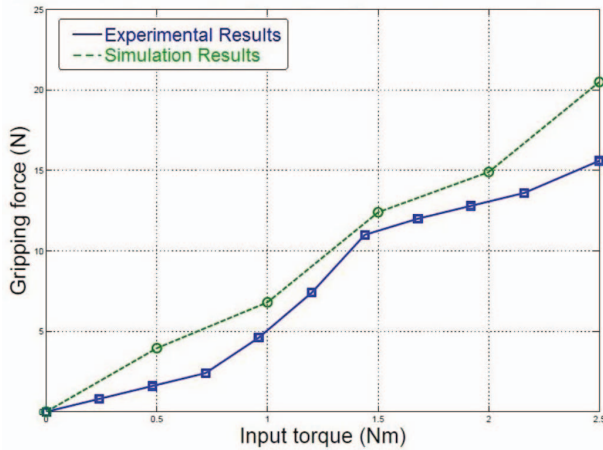


Fig. 9. The relationship of the grasping force versus input torque

TABLE I. COMPARISON OF ROBOTIC GRIPPERS

Hand	No. of fingers	No. of actuators	Gripping force (N)
Barrett Hand	3	4	15
Robotiq Adaptive Gripper	3	2	15-60
Schunk SDH Hand	3	7	-
Kinova JACO	3	3	-
SDM Hand	3	1	10
Proposed gripper	3	1	15

V. CONCLUSIONS AND FUTURE WORK

This paper presents author’s preliminary work on design of a 3D printed underactuated robotic gripper with the breakaway clutch mechanism. The presented robotic gripper design with one actuator is able to perform a wide range of grasping tasks and has advantages such as simple mechanical design, control system and potentially preferable in terms of the cost to payload ratio. The simplicity of the gripper elements and mechanisms allow their manufacturing with a 3D printing technology and additional off-the-shelf components. Theoretical expressions for calculated gripper design parameters are derived. The gripping force of the prototype is evaluated using computer simulation and experimental tests, whereas grasping performance is demonstrates using various shape objects. Comparison with widely applied and commercially available robotic end effectors shows the potential advantages of the proposed gripper design.

Future work includes design and implementation of proposed gripper prototype with embedded sensing elements such as tactile sensors for force feedback capabilities. The gripper will be mounted to an industrial manipulator for evaluating grasping performance in real-life scenarios.

REFERENCES

- [1] “Shadow Dexterous Hand Technical Specification,” 2013. [Online]. Available: http://www.shadowrobot.com/wp-content/uploads/shadow_dexterous_hand_technical_specification_E1_20130101.pdf.
- [2] S. Jacobsen, E. Iversen, D. Knutti, R. Johnson, and K. Biggers, “Design of the Utah/M.I.T. Dexterous Hand,” in *Proceedings. 1986 IEEE International Conference on Robotics and Automation*, 1986, vol. 3, pp. 1520–1532.
- [3] M. Baril, T. Laliberté, C. Gosselin, and F. Routhier, “On the Design of a Mechanically Programmable Underactuated Anthropomorphic Prosthetic Gripper,” *J. Mech. Des.*, vol. 135, no. 12, 2013.
- [4] T. Laliberté, L. Birglen, and C. Gosselin, “Underactuation in robotic grasping hands,” *Mach. Intell. Robot. Control*, vol. 4, no. 3, 2002.
- [5] A. Namiki, Y. Imai, M. Kaneko, and M. Ishikawa, “Development of a High-speed Multifingered Hand System,” *Proc. Int. Conf. Intell.*, no. October, pp. 2666–2671, 2004.
- [6] Schunk, “Servo-Electric 3-Finger Gripping Hand SDH.” [Online]. http://www.schunk.com/schunk_files/attachments/SDH_DE_EN.pdf.
- [7] W. Townsend, “The Barret Hand Grasper - Programmably Flexible Part Handling and Assembly,” *Ind. Rob.*, vol. 27, pp. 181–188, 2000.
- [8] L. U. L. Odhner, L. P. L. Jentoft, M. R. M. Claffee, N. Corson, Y. Tenzer, and R. Raymond, “A Compliant, Underactuated Hand for Robust Manipulation,” 2013. [Online]. Available: http://biorobotics.harvard.edu/pubs/2013/journal/2013_IJRR_i-HY.pdf. [Accessed: 05-Feb-2014].
- [9] T. U. Delft, “Delft Hand.” [Online]. Available: <http://www.3me.tudelft.nl/en/about-the-faculty/departments/biomechanical-engineering/research/dbl-delft-biorobotics-lab/delft-arm-and-hand/>.
- [10] Robotiq, “Three-Finger Adaptive Robot Gripper.” [Online]. Available: <http://robotiq.com/media/Robotiq-3-Finger-Adaptive-Robot-Gripper-Specifications.pdf>.
- [11] Kinova, “JACO Research Edition.” [Online]. Available: <http://kinovarobotics.com/wp-content/uploads/2013/05/kinova-jaco-spec-sheet.pdf>.
- [12] S. J. Bartholet, “Reconfigurable end effector,” *U.S. Patent 5 108 140*. 1992.
- [13] C. M. Gosselin, “Adaptive Robotic Mechanical Systems: A Design Paradigm,” *J. Mech. Des.*, vol. 128, no. 1, pp. 192–198, 2005.
- [14] T. Laliberté and C. Gosselin, “Actuation system for highly underactuated gripping mechanism,” *U.S. Patent 6 505 870*. 2003.
- [15] L. É. L. J. CARON and C. Deguire, “Mechanical Finger,” *PCT Patent WO2010/142043 A1*. 2010.
- [16] S. Montambault and C. M. Gosselin, “Analysis of Underactuated Mechanical Grippers,” *J. Mech. Des.*, vol. 123, no. 3, pp. 367–374, 2001.
- [17] L. Birglen and C. Gosselin, “Geometric design of three-phalanx underactuated fingers,” *J. Mech. Des.*, vol. 128, no. 2, pp. 356–364, 2005.
- [18] G. Figliolini and P. Rea, “Ca.U.M.Ha. robotic hand (Cassino-Underactuated-Multifinger-Hand),” *2007 IEEE/ASME international conference on advanced intelligent mechatronics*. Ieee, pp. 1–6, 2007.
- [19] L. Birglen and C. M. Gosselin, “Kinetostatic analysis of underactuated fingers,” *Robot. Autom. IEEE Trans.*, vol. 20, no. 2, pp. 211–221, 2004.
- [20] I. A. Bonev, D. Zlatanov, and C. M. Gosselin, “Singularity Analysis of 3-DOF Planar Parallel Mechanisms via Screw Theory,” *J. Mech. Des.*, vol. 125, no. 3, p. 573, 2003.
- [21] L. Birglen and C. M. Gosselin, “Force analysis of connected differential mechanisms: application to grasping,” *Int. J. Rob. Res.*, vol. 25, no. 10, pp. 1033–1046, 2006.
- [22] R. R. Ma, L. U. Odhner, and A. M. Dollar, “A modular, open-source 3D printed underactuated hand,” in *Robotics and Automation (ICRA), 2013 IEEE International Conference on*, 2013, pp. 2737–2743.
- [23] N. T. Ulrich, “Methods and apparatus for mechanically intelligent grasping,” *U.S. Patent 4 957 320*. 1990.
- [24] Robotis, “Dynamixel MX-28.” [Online]. Available: http://support.robotis.com/en/product/dynamixel/mx_series/mx-28.htm.
- [25] T. Laliberté and C. M. Gosselin, “Underactuation in space robotic hands,” in *Proceedings of the 6th International Symposium on Artificial and Robotics & Automation in Space: I-SAIRAS*, 2001.